Photon counting for axion interferometry

Haocun Yu,[1,*] Ohkyung Kwon,[2] Devendra K. Namburi,[3] Robert H. Hadfield,[3] Hartmut Grote,[4] and Denis Martynov[5]

[1]University of Vienna, Faculty of Physics, Vienna Center for Quantum Science and Technology (VCQ), Research Network for Quantum Aspects of Space Time (TURIS), Boltzmanngasse 5, Vienna 1090, Austria
[2]University of Chicago, Chicago, Illinois 60637, USA
[3]James Watt School of Engineering, University of Glasgow, University Avenue, Glasgow G12 8QQ, United Kingdom
[4]School of Physics and Astronomy, Cardiff University, Cardiff CF24 3AA, United Kingdom
[5]University of Birmingham, School of Physics and Astronomy, Birmingham B15 2TT, United Kingdom

(Received 15 December 2023; accepted 19 April 2024; published 24 May 2024)

Axions and axionlike particles are well-motivated dark matter candidates. We propose a novel experiment that uses single-photon detection interferometry to search for axions and axionlike particles in the Galactic halo. We show that photon counting with a dark count rate of 6×10^{-6} Hz can improve the quantum sensitivity of axion interferometry by a factor of 50 compared to the quantum-enhanced heterodyne readout for 5-m-long optical resonators. The proposed experimental method has the potential to be scaled up to kilometer-long facilities, enabling the detection or setting of constraints on the axion-photon coupling coefficient of $10^{-17} - 10^{-16}$ GeV^{-1} for axion masses ranging from 0.1 to 1 neV.

DOI: 10.1103/PhysRevD.109.095042

I. INTRODUCTION

There is substantial evidence from astrophysical [1–3] and cosmological [4] observations for the existence of dark matter. Among various extended theories beyond the Standard Model of particle physics, QCD axions [5–8] and pseudoscalar axionlike particles (ALPs) [9–11] are widely recognized as leading candidates.

We consider ALP dark matter to behave as a coherent, classical field a and interact weakly with photons through the coefficient $g_{a\gamma}$:

$$\mathcal{L} \subset -\frac{1}{4} g_{a\gamma} a F \tilde{F}. \tag{1}$$

This interaction induces a phase velocity difference between left- and right-handed circularly polarized light [12–15], which can be accumulated and extracted using a properly designed optical cavity and laser interferometry.

Several experiments were proposed in the literature to search for ALPs with interferometry [16–19], and the first results were recently published [20,21]. In previous work, the signal light is measured by beating the signal field with a strong local oscillator field. The advantage of this technique is that the measurement can be done with a standard photodetector with a high quantum efficiency. However, the readout suffers from quantum shot noise from the local oscillator field.

In this paper, we derive the sensitivity of axion interferometers using photon-counting detectors to directly detect the signal field, eliminating the need to beat it against the local oscillator field. We show their capacity to enhance detector sensitivity for axion fields with coherence times that are relatively short, especially when compared to the periods between dark counts of single-photon detectors. Over the past few decades, the technology for detecting single photons at near-infrared wavelengths has matured significantly [22–25]. The idea of employing single-photon detection was also introduced in the context of microwave cavity axion searches [26] and high-power interferometers for gravitational-wave detection [27]. Recent transition-edge sensors and superconducting nanowire single-photon detectors (SNSPDs) feature high detection efficiency exceeding 90% and exceptionally low dark count rates of 6×10^{-6} Hz [24,28–30]. This is a vast improvement on commercial-off-the-shelf InGaAs single-photon avalanche diodes, which, even if operated at 70 K, offer detection efficiency of 25% and minimum dark count rates of 50 per second [25]. The use of advanced superconducting detectors would extend the time intervals between detector dark count events, surpassing the coherence time of the axion field above 0.1 neV, and hold the potential to enhance the quantum-limited sensitivity of axion interferometers.

We analyse an axion interferometer which consists of a linear optical cavity and derive its optimal parameters for heterodyne and single-photon readouts. Our technique is also applicable to folded cavities. We calculate the signal-to-noise ratio for linear cavities of length from 1 m up to

*Corresponding author: haocunyu@mit.edu

10 km and show the advantage of single-photon detection compared to heterodyne readout in axion interferometry. The proposed approach has the potential to be integrated into both tabletop experiments and existing facilities for gravitational-wave detectors, such as GEO 600 [31] and LIGO facilities [32,33].

II. EXPERIMENTAL SETUP

Figure 1 shows the proposed axion interferometer with single-photon detection. A laser beam in P polarization (red) is injected into a high-finesse Fabry-Pérot linear cavity. To maximize the signal-to-noise ratio, the bandwidth of this main cavity is designed to match one of the axion fields (see Sec. III for a discussion on the bandwidth of the axion field). It is also beneficial to keep the cavity undercoupled ($T_2 > T_1$) to transmit most of the signal field to the readout port, where T_1 and T_2 are power transmissivities of the input and output coupler of the cavity. Because of the presence of the ALP field, the resonating laser field in P polarization undergoes partial conversion to S polarization (blue). The signal field around the free spectral range (f_{FSR}) of the cavity is further amplified by the optical resonance and transmitted through the output port. In other words, the detector is mostly resonantly sensitive to axion fields whose Compton frequency $f_a = m_a c^2/h$ is equal to $f_{\mathrm{FSR}} = c/(2L)$ or a multiple thereof.

When using the method of heterodyne readout, a small fraction of the pump field is converted to S polarization and used as a local oscillator for the readout [34]. For the proposed single-photon readout, the main challenge in the experiment is isolating S-polarization photons from the P-polarization ones in the pump field transmitting out of the cavity. The transmitted pump field has a photon rate of approximately 10^{20} Hz, which needs to be reduced to below 10^{-6} Hz to prevent false detections by the single-photon readout.

Because the pump and signal fields have orthogonal polarizations, a series of polarized optics, including polarizing beam splitters and linear polarizers with high extinction ratios, can be used to attenuate the transmitted pump field by 12–18 orders of magnitude. Commercial high-quality birefringent polarizers, such as Wollaston prisms, Glan-Taylor prisms, and nanoparticle linear film polarizers, have currently achieved extinction ratios of 10^7–10^8 : 1 [35]. Because of imperfections in the polarization optics, further suppression of the pump field is necessary. Since we are searching for axions at frequencies around the free spectral range of the main cavity, the signal fields are separated from the pump field in frequency as well. Accordingly, a triangular optical cavity with nondegenerate polarization modes can serve as a filter for both frequency and polarization in the final signal extraction. An odd number of cavity mirrors causes the P-polarization light to acquire an additional π phase and become off resonance. The polarization filtering extinction ratio increases as the square of the cavity finesse [36]. For a triangle cavity with a round-trip path length of 50 cm, assuming the input and output mirrors have the same transmittance of 100 ppm and a loss of 20 ppm, a finesse of 25000 can be achieved with a cavity bandwidth of 20 kHz. Comparable finesse and bandwidth have been demonstrated [37], and the proposed performance is promising with high-reflectance crystalline coatings [38,39]. When measuring the axion frequency around 10 MHz, this will theoretically provide up to 6 orders of magnitude suppression on the pump field due to the frequency difference and a polarization extinction ratio up to 8 orders of magnitude. Such a cavity can be controlled with auxiliary laser beams [40–42], and two or more such cavities in a series may be needed, depending on the performance of the upstream polarizing optics. Finally, an SNSPD with high system detection efficiency at 1064 nm wavelength plus a low dark count rate, enclosed in a 1 K cryostat, is used for signal detection. In particular, narrowband cold filtering tailored to the 1064 nm wavelength of this experiment will be employed to minimize the dark count rate [43–45].

III. SENSITIVITY AND INTEGRATION TIME

In this section, we show how single-photon detectors can improve the sensitivity of axion interferometers. In our experiment, the observable quantity is the phase difference accumulated by the left- and right-handed circularly polarized light that propagates in the presence of the axion field for a time period τ. The phase difference is given by the equation

$$\Delta\phi(t,\tau) = \sqrt{\hbar c}\, g_{a\gamma}[a(t) - a(t-\tau)], \tag{2}$$

where $\hbar$ is the reduced Planck constant, c is the speed of light, and $a(t)$ is the time-dependent amplitude of the axion field in the Galactic halo.

Now, we consider how linearly polarized light propagates in the axion field between two points separated by a distance L. We adopt Jones calculus with the electric field vector given by $(E_p, E_s)^T$, where E_p and E_s are the horizontal and vertical components of the field, respectively. The Jones matrix for the propagation of light in the axion field is given by the equation

$$A^{-1}\begin{pmatrix} e^{i\Delta\phi/2} & 0 \\ 0 & e^{-i\Delta\phi/2} \end{pmatrix} A \approx \begin{pmatrix} 1 & \Delta\phi/2 \\ -\Delta\phi/2 & 1 \end{pmatrix}, \tag{3}$$

where matrices A and its inverse A^{-1} convert electric fields from the linear basis to circular ones and back.

In further analysis, we neglect the time dependence of the pump field in the cavity $E_{s,\mathrm{cav}}$ because it is not affected by the axion field. The field in the S polarization builds up in the main cavity due to the axion field according to the equations

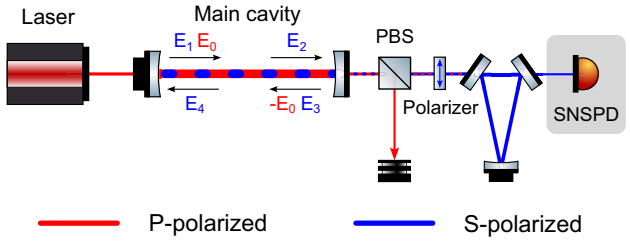

FIG. 1. Schematic of the experimental setup. P-polarized pump light resonates in a main linear optical cavity. The ALP field converts a small portion of light into S-polarized at a shifted frequency, which is isolated by a series of polarized optics and triangular optical cavities. The signal field is detected by an SNSPD. PBS: polarizing beam splitter.

$$\begin{aligned} E_2(t) &= E_1(t-\tau) - \frac{1}{2}\Delta\phi(t,\tau)E_0, \\ E_3(t) &= r_2 E_2(t), \\ E_4(t) &= E_3(t-\tau) + \frac{1}{2}\Delta\phi(t,\tau)E_0, \\ E_1(t) &= r_1 E_4(t), \end{aligned} \tag{4}$$

where τ is the single-trip travel time in the cavity; r_1 and r_2 are the field reflectivities of the input and output couplers; E_0 is the pump field forward propagating within the main linear cavity, with its sign flipped by the output coupler; $E_{1\text{–}4}$ are S-polarization electric fields propagating within the cavity near the input (E_1 and E_4) and output (E_2 and E_3) couplers (see Fig. 1). Solving Eq. (4) relative to E_2 and neglecting the factors r_1 and r_2 under the approximation r_1, $r_2 \approx 1$ in the driving term, we get

$$E_2(t) = r_1 r_2 E_2(t-2\tau) - \frac{E_0}{2}\big(\Delta\phi(t,\tau) - \Delta\phi(t-\tau,\tau)\big). \tag{5}$$

If dark matter consists of ALPs with mass m_a, then its field behaves classically and can be written as [46]

$$a(t) = a_0 \sin(\Omega_a t + \delta(t)), \tag{6}$$

where the angular frequency $\Omega_a = 2\pi f_a = m_a c^2/\hbar$; $a_0 = \sqrt{2\rho_{\rm DM}}\hbar/m_a$ is the amplitude of the field, with $\rho_{\rm DM} \approx 0.3$ GeV/cm^3 as the local density of dark matter; $\delta(t)$ is the phase offset of the field. The phase offset remains constant for times $t \lesssim \tau_a$, where $\tau_a = Q_a/f_a$ is the coherence time of the field, $Q_a = c^2/v^2 \sim 10^6$ is the quality factor of the oscillating field, and v is the Galactic virial velocity of the ALP dark matter [9]. Equation (6) neglects spatial variations of the field, since ALP wavelength $\lambda_a > 100$ km is significantly larger than the length of the proposed experiment for $m_a < 10^{-8}$ eV.

By setting the cavity single-trip time to $\Omega_a\tau = \pi$ (i.e., the axion mass is appropriately resonant with the cavity) and applying Eqs. (2) and (6), Eq. (5) can be simplified to

$$E_2(t) = r_1 r_2 E_2(t-2\tau) - 2E_0 a(t) g_{a\gamma}\sqrt{\hbar c}. \tag{7}$$

Since the phase of the axion field stays constant much longer than τ, the solution for the field transmitted to the readout port is given by the equation

$$\begin{aligned} E_{\rm out}(t) = \sqrt{T_2}E_2(t) &\approx E_0 \frac{2\sqrt{T_2}}{r_1 r_2 - 1} a(t) g_{a\gamma}\sqrt{\hbar c} \\ &\approx E_0 G\theta(t), \end{aligned} \tag{8}$$

where $G = 2\sqrt{T_2}/(r_1 r_2 - 1)$ represents the cavity gain; $\theta = a(t)g_{a\gamma}\sqrt{\hbar c} \ll 1$ is the conversion efficiency of the pump field to the signal field in the presence of the axion field.

We now consider the signal-to-noise ratio accumulated with two types of readout methods: heterodyne and single-photon counting. For the heterodyne readout, we intend to install a half-wave plate in the transmission path of the cavity to convert a fraction of the transmitted pump field to the local oscillator field $E_{\rm LO}$ [19,34]. The time-dependent component of the power observed on a photodetector is then given by the equation

$$P_h(t) = 2E_{\rm LO}E_{\rm out}(t) = 2\sqrt{P_{\rm LO}P_0}G\theta(t). \tag{9}$$

The single-sided power spectral density of $P_h(t)$ around the frequency of the axion field Ω_a is given by the equation

$$S_{PP} = 16 P_{\rm LO}P_0 G^2 \frac{g_{a\gamma}^2 \rho_{\rm DM}\hbar c^5}{\Omega_a^2} T, \tag{10}$$

where $T = \min(T_{\rm int}, \tau_a)$ and $T_{\rm int} \gg \tau$ is the integration time. For $T_{\rm int} < \tau_a$, we set our frequency spacing in the power spectral density estimation to $1/T_{\rm int}$, and the peak in S_{PP} at frequency Ω_a grows linearly with time. For $T_{\rm int} \geq \tau_a$, the peak of the axion field is resolved, and the power spectral density does not grow for a larger integration time. However, the signal-to-noise ratio still improves for $T_{\rm int} \geq \tau_a$, because we can subtract the mean value of the shot noise with higher precision. The single-sided power spectral density of the shot noise is given by the equation

$$S_{\rm shot} = \frac{2\hbar\omega_0 P_{\rm LO}e^{-2r}}{\sqrt{K}}, \tag{11}$$

where ω_0 is the angular frequency of the laser light; r is the squeezing factor [47,48]; and $K = \max(1, T_{\rm int}/\tau_a)$ is the number of power spectral density averages that can be made with optimal frequency resolution: $1/T_{\rm int}$ for $T_{\rm int} < \tau_a$ and $1/\tau_a$ for $T_{\rm int} \geq \tau_a$. The signal-to-noise ratio is then given by the equation

$$\mathrm{SNR}_h^2 = \frac{S_{PP}}{S_{\mathrm{shot}}} = \frac{4P_0G^2g_{a\gamma}^2\rho_{\mathrm{DM}}c^4\lambda e^{2r}}{\pi\Omega_a^2}\sqrt{T_{\mathrm{int}}T}, \quad (12)$$

where λ is the wavelength of light.

In the case of photon counting, we observe only signal fields by rejecting the pump field in the orthogonal direction with polarization optics and mode cleaners as discussed in Sec. II. The time-averaged power on the single-photon detector is then given by the equation

$$P_c = P_0G^2g_{a\gamma}^2\frac{4\rho_{\mathrm{DM}}\hbar c^5}{\Omega_a^2}, \quad (13)$$

and the time-averaged number of photons observed during the integration time T_{int} is given by the equation

$$N = \frac{P_cT_{\mathrm{int}}}{\hbar\omega_0} = P_0G^2g_{a\gamma}^2\frac{2\rho_{\mathrm{DM}}c^4\lambda}{\pi\Omega_a^2}T_{\mathrm{int}}. \quad (14)$$

We do not suffer from shot noise from the local oscillator while counting photons. However, single-photon detectors observe dark counts with a time constant τ_d. For state-of-the-art single-photon detectors, τ_d is on the order of 10^5 s. If integration time $T_{\mathrm{int}} = Q\tau_d$, we expect Q dark clicks of our detector with the standard deviation of $\sqrt{Q}$. Therefore, the signal-to-noise ratio is given by the equation

$$\mathrm{SNR}_c^2 = \frac{N}{\sqrt{Q}} = \frac{2P_0G^2g_{a\gamma}^2\rho_{\mathrm{DM}}c^4\lambda}{\pi\Omega_a^2}\sqrt{T_{\mathrm{int}}T_d}, \quad (15)$$

where $T_d = \min(T_{\mathrm{int}}, \tau_d)$.

Comparing the signal-to-noise ratios from Eqs. (12) and (15), we find that an improvement in the estimation of $g_{a\gamma}$ can be achieved if $\tau_d \gg \tau_a$. The improvement factor is given by the equation

$$\frac{\mathrm{SNR}_c}{\mathrm{SNR}_h} = \frac{1}{\sqrt{2}e^r}\left(\frac{\tau_d}{\tau_a}\right)^{1/4} \approx \frac{1}{\sqrt{2}e^r}\left(\frac{\tau_d f_a}{Q_a}\right)^{1/4}. \quad (16)$$

Figure 2 compares the limits on $g_{a\gamma}$ that linear cavities can achieve with heterodyne (blue) and photon counting detectors (red), based on Eqs. (12) and (15) with $\mathrm{SNR}_{c,h} = 1$. The cavity length is tuned for each frequency of the axion field $f_a = c/2L$ to satisfy the condition $\Omega_a\tau = \pi$. Based on the 5-m-long laser-interferometric detector for axions (LIDA) with 120 kW resonating power [21], we assume the power transmissivity of the cavity output coupler $T_2 = T_1 + Y$, where $Y = 1.7$ ppm $\times \sqrt{L/5\ \mathrm{m}}$ is the round-trip loss in a cavity of length L. We also impose $T_2 > 3$ ppm to ensure that the cavity bandwidth is larger than the bandwidth of the axion field. We assume the resonating power of $P_0 = \min(120\ \mathrm{kW} \times L/5\ \mathrm{m}, 10\ \mathrm{MW})$. Since the beam area size increases with the cavity length, the laser intensity on the mirrors remains constant when the cavity length and resonating power are increased by the same factor. The upper limit of 10 MW is chosen to accommodate the technical complexities associated with maintaining high-quality coatings over large surface areas. For heterodyne readout, we assume the injection of 10 dB squeezing when the cavity is less than 10 m for quantum enhancement [34]. Squeezing for longer cavities becomes obsolete, because the squeezing efficiency decreases with increasing cavity length due to cavity loss. For photon counting, we assume an integration time T_{int} of 100 days and $\tau_d = 1.5 \times 10^5$ s. Over long experimental run-times, studying the stochastic fluctuations in the time-series data may also help eliminate background noises and reveal signatures of ALP particles with masses on the order of neV [49].

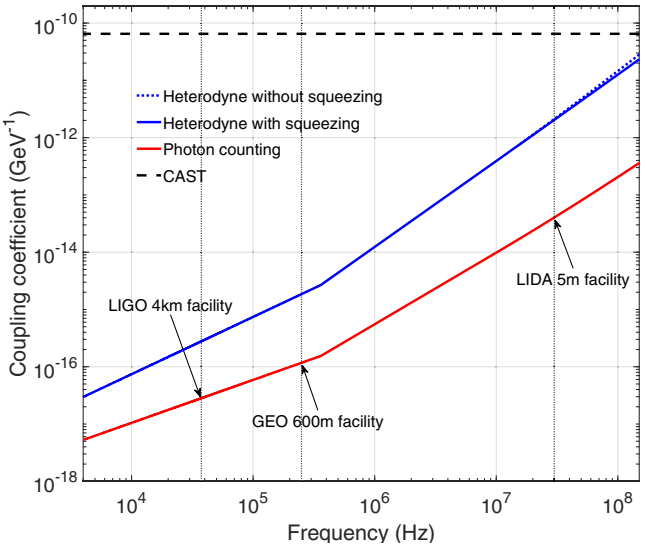

FIG. 2. Estimated limits on the axion-photon coupling coefficients using photon-counting readout, compared with those obtained through heterodyne readout. Each curve shows the enveloped sensitivities of different fixed-length detectors at specific axion masses. For example, the LIGO 4-km facility has a sensitivity bandwidth of 0.3 Hz centered around 37.5 kHz. The "kink" in each curve around 5×10^5 Hz ($L \approx 400$ m) originates from the assumption that the resonating power of the cavity increases linearly with the cavity length but remains constant after reaching the upper limit of 10 MW. The existing limit from the CERN Axion Solar Telescope (CAST) [50] is shown as a reference.

Taking the 5-m LIDA detector as an example, an improvement factor of 50 can be achieved with photon counting compared to the heterodyne readout when measuring $g_{a\gamma}$ at 30 MHz ($m_a = 124$ neV). The length of the GEO 600 facility corresponds to an axion frequency of 250 kHz ($m_a = 1$ neV), resulting in an improvement factor of 16. For a 4-km detector that can be installed in the LIGO facilities, the improvement factor would be 10 for an axion frequency of 37.5 kHz ($m_a = 0.15$ neV).

We also note that the sensitivity curves in Fig. 2 are calculated for a light wavelength $\lambda = 1064$ nm. According to Eq. (15), the SNR scales as $\sqrt{\lambda}$, suggesting that longer wavelengths lead to an improvement in the $g_{a\gamma}$ constraints. In the case of microwave photons ($\tau_a \sim 10^{-3}$ s), using a 5-m-long gigahertz resonator similar to the ADMX one [51] and a microwave single-photon detector with low dark count rate [52,53] ($\tau_d > 10$ s) has the potential to probe axion fields around 100 neV down to $g_{a\gamma} \approx 10^{-16}$ GeV^{-1}.

IV. CONCLUSION

In this work, we proposed an axion interferometer with single-photon counting methods targeting to detect or set constraints for axion-photon coupling coefficient for axion masses of 0.1–100 neV. Looking into the future, current gravitational-wave facilities are potential infrastructures to be transformed into axion interferometers, given their existing high-power lasers, ultrastable linear optical cavities, and vacuum envelopes. The proposed configuration and techniques also have the potential to be extended to an interferometric experiment for estimating gradients in the static axion field [54].

The photon-counting technique holds great promise for surpassing the quantum shot-noise limit, which represents the fundamental noise floor in existing experiments. A key challenge is separating the intense pump field from the faint signal field. This can be addressed by installing polarization optics and a set of mode cleaners in the readout path. However, classical noise sources, such as technical laser noise and electronic noise, can also impose limitations on the sensitivity [20,21]. Similar to other experiments based on birefringence in optical cavities [55], spurious signals may arise due to scattered light and misalignment of polarized optics caused by mechanical vibrations and acoustic noise. Moreover, we note that the sensitivity of the axion interferometer with photon readout is currently limited by the dark rate of state-of-the-art single-photon detectors. Anticipated advancements in single-photon detector technologies will lead to enhanced constraints on the axion-photon coupling parameter $g_{a\gamma}$.

Finally, we computed the sensitivity curve for both heterodyne and single-photon readout across resonator lengths ranging from 1 m to 10 km. The scaling of the SNR improvement will be similar for folded resonators as long as the dark count rate is lower than the bandwidth of the axion field. The scaling is also applicable for gigahertz resonators, which have the potential to probe the axion-photon interaction at a deeper level than constraining $g_{a\gamma}$ with optical resonators.

ACKNOWLEDGMENTS

We acknowledge the support of the Quantum Interferometry Collaboration for useful discussions. H. Y. acknowledges support from the Marie-Skłodowska Curie Postdoctoral Fellowship program hosted by the Horizon Europe (Grant No. 101064373). O. K. and H. G. acknowledge support from UKRI Science and Technology Facilities Council (STFC) under Grant No. ST/Y005082/1. H. G. and D. M. acknowledge the support of STFC Quantum Technology for Fundamental Physics scheme (Grants No. ST/T006609/1, No. ST/W006375/1, and No. ST/T006331/1). D. M. further acknowledges the Institute for Gravitational Wave Astronomy at the University of Birmingham. D. M. is supported by the 2021 Philip Leverhulme Prize.

[1] Y. Sofue and V. Rubin, Rotation curves of spiral galaxies, Annu. Rev. Astron. Astrophys. **39**, 137 (2001).
[2] M. Markevitch, A. H. Gonzalez, D. Clowe, A. Vikhlinin, W. Forman, C. Jones, S. Murray, and W. Tucker, Direct constraints on the dark matter self-interaction cross section from the merging galaxy cluster 1e 0657-56, Astrophys. J. **606**, 819 (2004).
[3] R. Massey, T. Kitching, and J. Richard, The dark matter of gravitational lensing, Rep. Prog. Phys. **73**, 086901 (2010).
[4] G. Bertone, D. Hooper, and J. Silk, Particle dark matter: Evidence, candidates and constraints, Phys. Rep. **405**, 279 (2005).
[5] R. D. Peccei and H. R. Quinn, CP conservation in the presence of pseudoparticles, Phys. Rev. Lett. **38**, 1440 (1977).
[6] J. Preskill, M. B. Wise, and F. Wilczek, Cosmology of the invisible axion, Phys. Lett. **120B**, 127 (1983).
[7] L. F. Abbott and P. Sikivie, A cosmological bound on the invisible axion, Phys. Lett. **120B**, 133 (1983).
[8] M. Dine and W. Fischler, The not so harmless axion, Phys. Lett. **120B**, 137 (1983).
[9] P. W. Graham and S. Rajendran, New observables for direct detection of axion dark matter, Phys. Rev. D **88**, 035023 (2013).
[10] A. Ringwald, Exploring the role of axions and other wisps in the dark universe, Phys. Dark Universe **1**, 116 (2012), next Decade in Dark Matter and Dark Energy.
[11] P. Svrcek and E. Witten, Axions in string theory, J. High Energy Phys. 06 (2006) 051.

[12] S. M. Carroll, G. B. Field, and R. Jackiw, Limits on a Lorentz- and parity-violating modification of electrodynamics, Phys. Rev. D **41**, 1231 (1990).
[13] S. M. Carroll and G. B. Field, Einstein equivalence principle and the polarization of radio galaxies, Phys. Rev. D **43**, 3789 (1991).
[14] D. Harari and P. Sikivie, Effects of a Nambu-Goldstone boson on the polarization of radio galaxies and the cosmic microwave background, Phys. Lett. B **289**, 67 (1992).
[15] S. M. Carroll, Quintessence and the rest of the world: Suppressing long-range interactions, Phys. Rev. Lett. **81**, 3067 (1998).
[16] A. C. Melissinos, Proposal for a search for cosmic axions using an optical cavity, Phys. Rev. Lett. **102**, 202001 (2009).
[17] I. Obata, T. Fujita, and Y. Michimura, Optical ring cavity search for axion dark matter, Phys. Rev. Lett. **121**, 161301 (2018).
[18] W. DeRocco and A. Hook, Axion interferometry, Phys. Rev. D **98**, 035021 (2018).
[19] H. Liu, B. D. Elwood, M. Evans, and J. Thaler, Searching for axion dark matter with birefringent cavities, Phys. Rev. D **100**, 023548 (2019).
[20] Y. Oshima, H. Fujimoto, J. Kume, S. Morisaki, K. Nagano, T. Fujita, I. Obata, A. Nishizawa, Y. Michimura, and M. Ando, First results of axion dark matter search with DANCE, Phys. Rev. D **108**, 072005 (2023).
[21] J. Heinze, A. Gill, A. Dmitriev, J. Smetana, T. Yan, V. Boyer, D. Martynov, and M. Evans, First results of the laser-interferometric detector for axions (LIDA), Phys. Rev. Lett. **132**, 191002 (2024).
[22] M. Eisaman, J. Fan, A. Migdall, and S. Polyakov, Invited review article: Single-photon sources and detectors, Rev. Sci. Instrum. **82**, 071101 (2011).
[23] I. Esmaeil Zadeh, J. Chang, J. Los, S. Gyger, A. W. Elshaari, S. Steinhauer, S. Dorenbos, and V. Zwiller, Superconducting nanowire single-photon detectors: A perspective on evolution, state-of-the-art, future developments, and applications, Appl. Phys. Lett. **118**, 190502 (2021).
[24] A. C. Dmitry V. Morozov and R. H. Hadfield, Superconducting photon detectors, Contemp. Phys. **62**, 69 (2021).
[25] R. H. Hadfield, J. Leach, F. Fleming, D. J. Paul, C. H. Tan, J. S. Ng, R. K. Henderson, and G. S. Buller, Single-photon detection for long-range imaging and sensing, Optica **10**, 1124 (2023).
[26] S. K. Lamoreaux, K. A. van Bibber, K. W. Lehnert, and G. Carosi, Analysis of single-photon and linear amplifier detectors for microwave cavity dark matter axion searches, Phys. Rev. D **88**, 035020 (2013).
[27] L. McCuller, Single-photon signal sideband detection for high-power Michelson interferometers, arXiv:2211.04016.
[28] F. Marsili, V. B. Verma, J. A. Stern, S. Harrington, A. E. Lita, T. Gerrits, I. Vayshenker, B. Baek, M. D. Shaw, R. P. Mirin, and S. W. Nam, Detecting single infrared photons with 93% system efficiency, Nat. Photonics **7**, 210 (2013).
[29] D. V. Reddy, R. R. Nerem, S. W. Nam, R. P. Mirin, and V. B. Verma, Superconducting nanowire single-photon detectors with 98% system detection efficiency at 1550 nm, Optica **7**, 1649 (2020).
[30] V. Verma, B. Korzh, A. Walter, A. Lita, R. Briggs, M. Colangelo, Y. Zhai, E. Wollman, A. Beyer, J. Allmaras, H. Vora, D. Zhu, E. Schmidt, A. Kozorezov, K. Berggren, R. Mirin, S. Nam, and M. Shaw, Single-photon detection in the mid-infrared up to 10 um wavelength using tungsten silicide superconducting nanowire detectors, APL Photonics **6**, 056101 (2021).
[31] H. Grote and (LIGO Scientific Collaboration), The GEO 600 status, Classical Quantum Gravity **27**, 084003 (2010).
[32] B. P. Abbott *et al.*, LIGO: The laser interferometer gravitational-wave observatory, Rep. Prog. Phys. **72**, 076901 (2009).
[33] B. P. Abbott *et al.* (LIGO Scientific and Virgo Collaborations), GW150914: The Advanced LIGO detectors in the era of first discoveries, Phys. Rev. Lett. **116**, 131103 (2016).
[34] D. Martynov and H. Miao, Quantum-enhanced interferometry for axion searches, Phys. Rev. D **101**, 095034 (2020).
[35] R. Paschotta, *Polarizers* (RP Photonics AG, 2012), 10.61835/7ae.
[36] F. Raab and S. Whitcomb, Estimation of special optical properties of a triangular ring cavity, Report No. LIGO-T920004-00-R (1992).
[37] P. Kwee, C. Bogan, K. Danzmann, M. Frede, H. Kim, P. King, J. Pöld, O. Puncken, R. L. Savage, F. Seifert, P. Wessels, L. Winkelmann, and B. Willke, Stabilized high-power laser system for the gravitational wave detector Advanced LIGO, Opt. Express **20**, 10617 (2012).
[38] G. Cole, W. Zhang, M. Martin, J. Ye, and M. Aspelmeyer, Tenfold reduction of Brownian noise in high-reflectivity optical coatings, Nat. Photonics **7**, 644 (2013).
[39] D. Kedar, J. Yu, E. Oelker, A. Staron, W. R. Milner, J. M. Robinson, T. Legero, F. Riehle, U. Sterr, and J. Ye, Frequency stability of cryogenic silicon cavities with semiconductor crystalline coatings, Optica **10**, 464 (2023).
[40] A. Staley *et al.*, Achieving resonance in the Advanced LIGO gravitational-wave interferometer, Classical Quantum Gravity **31**, 245010 (2014).
[41] K. Izumi, K. Arai, B. Barr, J. Betzwieser, A. Brooks, K. Dahl, S. Doravari, J. C. Driggers, W. Z. Korth, H. Miao, J. Rollins, S. Vass, D. Yeaton-Massey, and R. X. Adhikari, Multicolor cavity metrology, J. Opt. Soc. Am. A **29**, 2092 (2012).
[42] A. J. Mullavey, B. J. J. Slagmolen, J. Miller, M. Evans, P. Fritschel, D. Sigg, S. J. Waldman, D. A. Shaddock, and D. E. McClelland, Arm-length stabilisation for interferometric gravitational-wave detectors using frequency-doubled auxiliary lasers, Opt. Express **20**, 81 (2012).
[43] H. Shibata, H. T. Kaoru Shimizu, and Y. Tokura, Ultimate low system dark-count rate for superconducting nanowire single-photon detector, Opt. Lett. **40**, 3428 (2015).
[44] W. Zhang, X. Yang, H. Li, L. You, C. Lv, L. Zhang, C. Zhang, X. Liu, Z. Wang, and X. Xie, Fiber-coupled superconducting nanowire single-photon detectors integrated with a bandpass filter on the fiber end-face, Supercond. Sci. Technol. **31**, 035012 (2018).
[45] A. S. Mueller, M. R. Boris Korzh, E. E. Wollman, A. D. Beyer, J. P. Allmaras, A. E. Velasco, I. Craiciu, B. Bumble, R. M. Briggs, L. Narvaez, C. Peña, M. Spiropulu, and M. D. Shaw, Free-space coupled superconducting nanowire single-photon detector with low dark counts, Optica **8**, 1586 (2021).

[46] D. Budker, P. W. Graham, M. Ledbetter, S. Rajendran, and A. O. Sushkov, Proposal for a cosmic axion spin precession experiment (casper), Phys. Rev. X **4**, 021030 (2014).
[47] B. L. Schumaker and C. M. Caves, New formalism for two-photon quantum optics. II. Mathematical foundation and compact notation, Phys. Rev. A **31**, 3093 (1985).
[48] R. Schnabel, Squeezed states of light and their applications in laser interferometers, Phys. Rep. **684**, 1 (2017).
[49] J. W. Foster, N. L. Rodd, and B. R. Safdi, Revealing the dark matter halo with axion direct detection, Phys. Rev. D **97**, 123006 (2018).
[50] CAST Collaboration, New cast limit on the axion–photon interaction, Nat. Phys. **13**, 584 (2017).
[51] N. Du *et al.* (ADMX Collaboration), Search for invisible axion dark matter with the axion dark matter experiment, Phys. Rev. Lett. **120**, 151301 (2018).
[52] A. V. Dixit, S. Chakram, K. He, A. Agrawal, R. K. Naik, D. I. Schuster, and A. Chou, Searching for dark matter with a superconducting qubit, Phys. Rev. Lett. **126**, 141302 (2021).
[53] A. L. Pankratov, L. S. Revin, A. V. Gordeeva, A. A. Yablokov, L. S. Kuzmin, and E. Il'ichev, Towards a microwave single-photon counter for searching axions, npj Quantum Inf. **8**, 61 (2022).
[54] M. A. Fedderke, J. O. Thompson, R. Cervantes, B. Giaccone, R. Harnik, D. E. Kaplan, S. Posen, and S. Rajendran, Measuring axion gradients with photon interferometry, Phys. Rev. D **109**, 015025 (2024).
[55] A. Ejlli, F. Della Valle, U. Gastaldi, G. Messineo, R. Pengo, G. Ruoso, and G. Zavattini, The PVLAS experiment: A 25 year effort to measure vacuum magnetic birefringence, Phys. Rep. **871**, 1 (2020).